Energy Transfer in Spectrally Inhomogeneous Light-Harvesting Pigment–Protein Complexes of Purple Bacteria

S. Hess,* E. Åkesson,‡ R.J. Cogdell,§ T. Pullerits,* and V. Sundström*

*Department of Chemical Physics, Lund University, S-221 00 Lund, Sweden; ‡Department of Physical Chemistry, Umeå University, S-901 87 Umeå, Sweden; and §Division of Biochemistry and Molecular Biology, Glasgow University, Glasgow G12 8QQ, UK

ABSTRACT Energy transfer within the peripheral light-harvesting antenna of the purple bacteria *Rhodobacter sphaeroides* and *Rhodopseudomonas palustris* was studied by one- and two-color pump–probe absorption spectroscopy with ~100-fs tunable pulses at room temperature and at 77 K. The energy transfer from B800 to B850 occurs with a time constant of 0.7 ± 0.05 ps at room temperature and 1.8 ± 0.2 ps at 77 K and is similar in both species. Anisotropy measurements suggest a limited but fast B800 ↔ B800 transfer time ($\tau \sim 0.3$ ps). This is analyzed as incoherent hopping of the excitation in a system of spectrally inhomogeneous antenna pigment–protein complexes, by a master equation approach. The simulations show that the measured B800 dynamics is well described as energy transfer with a characteristic average nearest-neighbor pairwise transfer time of 0.35 ps among ~10 Bchl molecules in a circular arrangement, in good agreement with the recent high-resolution structure of LH2. The possible presence of fast intramolecular relaxation processes within the Bchl *a* molecule was investigated by measurement of time-resolved difference absorption spectra and kinetics of Bchl *a* in solution and in low-temperature glasses. From these measurements it is concluded that fast transients observed at room temperature are due mainly to solvation processes, whereas at 77 K predominantly slower (>10-ps) relaxation occurs.

INTRODUCTION

We report the time-resolved study of two purple bacteria, *Rhodobacter (Rb.) sphaeroides* and *Rhodopseudomonas (Rps.) palustris*. These photosynthetic bacteria hold two light-harvesting antenna systems, a peripheral antenna (LH2) and a core antenna (LH1), which surround the reaction center. The LH2 antenna has absorption maxima at 800 and 850 nm (usually designated B800 and B850), and the absorption band of the LH1 antenna has a maximum at 875 nm. Several biochemical, spectroscopic, and electron microscopy studies have given insight into the polypeptide organization in vivo (Kramer et al., 1984a,b; Hunter et al., 1988; Braun and Scherz, 1991; Visschers et al., 1991; Boonstra et al., 1993). Most spectral properties could be explained with an $(\alpha\beta)_2$ unit holding two Bchl 800, four Bchl 850, and three carotenoid molecules. The different absorption bands of these pigment–protein complexes originate from interactions between Bchl molecules and the distinctive protein surrounding of the pigment molecules. Very recently the three-dimensional structure of a LH2 complex from *Rps. acidophila* was solved to high resolution (McDermott et al., 1995), showing a ninefold circular symmetry of $\alpha\beta$ pairs. It will be interesting to analyze in the future the detailed role of this highly symmetric unit in the energy transfer of the LH2 antenna.

Energy transfer in photosynthetic purple bacteria has been extensively investigated by picosecond (Borisov et al., 1985; Sundström et al., 1986; Bergström et al., 1986; Van Grondelle et al., 1987; Bergström et al., 1988; Freiberg et al., 1989; Shimada et al., 1989; Timpmann et al., 1991; Sundström and van Grondelle, 1992; Zhang et al., 1992; Visscher et al., 1993) and more recently by femtosecond (Hess et al., 1993; Chachisvilis et al., 1994) time-resolved spectroscopy. In particular, B800 to B850 energy transfer in the light-harvesting antenna of *Rb. sphaeroides* has been thoroughly studied (Shreve et al., 1991; Hess et al., 1994).

With picosecond pulses it was concluded that the B800→850 energy transfer in *Rb. sphaeroides* occurs on a picosecond time scale and is temperature dependent; at room temperature it occurs with a characteristic time constant of ~1 ps, and it becomes somewhat slower (~2 ps) at 77 K (Sundström et al., 1986; Freiberg et al., 1989; Bergström et al., 1986; van Grondelle et al., 1987). Shreve et al. (1991) measured the rise time of the B850 bleaching after excitation of B800 in a LH2 complex of *Rb. sphaeroides*, but, because of the relatively high excitation density used in their experiment, the rise-time kinetics were distorted by singlet–singlet annihilation within the B850 antenna, and they were able to obtain only an estimate of the B800→B850 transfer time as >0.4 ps. Combining this result with the 0.7-ps decay time that they measured for the B800 excited state, these authors concluded that the energy transfer from B800 to B850 occurs with a 0.7-ps time constant at room temperature. In the measurements by Shreve et al. (1991) the rise time of the B850 excited state was probed at only one wavelength. However, in probing this rise time following B800 excitation it is also necessary to consider the internal dynamics of B850 to obtain a complete picture of the B800→B850 transfer. This can be done by probing the B850 dynamics over a wide range of wavelengths. More recent time-resolved measurements with

Received for publication 25 April 1995 and in final form 21 July 1995.

Address reprint requests to Dr. Villy Sundstrom, Department of Chemical Physics, University of Lund, P.O. Box 124, S-22100 Lund, Sweden. Tel.: 46-46-222-4690; Fax: 46-46-222-4848; E-mail: villy.sundstrom@chemphys.lu.se.

0006-3495/95/12/2211/15 $2.00

~100-fs resolution gave values of the B800 excited-state (B800*) decay time of 0.6 ± 0.1 ps at room temperature and 2.4 ± 0.4 ps at 77 K (Sundström and van Grondelle, 1992; Hess et al., 1993). Hole-burning experiments at ~4K yielded B800* lifetimes similar to those obtained from time-resolved experiments at 77 K; hole widths corresponding to 2.3–2.5 ps were reported by Van der Laan et al. (1990, 1993), Reddy et al. (1991), and de Caro et al. (1994).

The extent of B800 ↔ B800 energy transfer has been much more difficult to resolve because of the short excited-state lifetime of B800. Picosecond measurements at 77 K suggested only little B800 ↔ B800 energy transfer (van Grondelle et al., 1987), whereas steady-state fluorescence polarization measurements with Q_x excitation at 4 K indicated extensive depolarization of the B800 excited state (Kramer et al., 1984a). Measurements at room temperature with ~100-fs resolution showed that depolarization within B800 occurs with a time constant of 0.8–1.5 ps (Hess et al., 1993). In these measurements a very fast ~0.3-ps decay was also observed in the isotropic kinetics, which appeared to have no counterpart in the anisotropy decay. It was therefore suggested that this fast phase could correspond to vibrational relaxation or energy transfer between close-to-parallel B800 molecules, whereas additional B800 ↔ B800 transfer occurs with the slower time constant 0.8–1.5 ps. The nonexponential B800 excited-state decay kinetics (Hess et al., 1993) and wavelength-dependent hole widths in the hole-burning experiments (de Caro et al., 1994) make the unambiguous assignment of the B800 excited-state decay times to B800→B850 energy transfer difficult. The additional faster decay component could, e.g., be due to a heterogeneous B800→B850 and/or B800 ↔ B800 energy transfer from a spectrally inhomogeneous B800 or to other (non-energy-transfer-related) relaxation processes, e.g., vibrational relaxation, within B800. In addition, the fundamental difficulties in fitting of multiexponential decay curves (James and Ware, 1985) make it problematic to extract unambiguous lifetimes out of complex experimental data.

To obtain a clear assignment of the energy-transfer processes within LH2 from this kind of time-resolved experiment it is therefore necessary to measure the kinetics over a wide spectral range and at sufficiently low excitation energy to avoid singlet–singlet (van Grondelle, 1985) and singlet–triplet (Valkunas et al., 1991) annihilation. With the intention of unequivocally determining the pathways of energy transfer within the LH2 complex and the characteristic time constants for each process, we have performed femtosecond transient absorption measurements probing the dynamics in both the B800 and the B850 absorption bands, following excitation of B800 at room temperature and at 77 K. Measurements were also performed on Bchl *a* in solution and in low-temperature glasses to examine the possible influence of solvation dynamics and vibrational relaxation on the measured kinetics. The present experiments combined with computer simulations of the energy equilibration within B800 allow us to characterize the B800→B850 transfer process, the energy equilibration within B800, and the consequences of spectral inhomogeneity for the energy-transfer dynamics.

This paper is structured as follows: The experimental procedures are outlined, and then we describe and discuss the results of measurements on Bchl *a* in solution and in low-temperature glasses. The energy transfer from B800 to B850 is thoroughly examined in one- and two-color experiments. We describe various experimental results pertinent to the dynamics within B800 and perform the computer simulations of the same process. We conclude with a discussion of the results.

MATERIALS AND METHODS

Both one- and two-color femtosecond pump–probe measurements were performed in four different experimental arrangements. One set of measurements was based on the low-energy nanojoule and high-repetition-rate tunable infrared pulses from a mode-locked Ti:sapphire laser, and another measurement setup used the visible amplified microjoule 1-kHz pulses from a dye laser system.

Low-energy transient absorption with sub-100-fs resolution

To gain further knowledge concerning the energy transfer and relaxation process within B800 we measured the B800 kinetics in two slightly different absorption pump–probe experiments, using either spectrally integrated or dispersed detection of the probe. For both measurements an argon-ion laser delivering 11 W of power was used to pump a self-mode-locked Ti:sapphire laser with tunability in the spectral region 720–850 nm. With this system ~80-fs pulses at a 82-MHz repetition rate and 1-W output power were generated. To reduce accumulation of long-lived photoproducts and heating of the sample, the pulse repetition rate was decreased to 800 kHz with an acousto-optic pulse selector; and to avoid damage to the Bragg cell in the pulse selector the pulses were first stretched to ~300 fs. After the pulse selector the pulses were recompressed with a home-built compressor, which consists of a pair of SF-10 dispersion prisms. The resulting pulses had an ~100-fs autocorrelation with a spectral bandwidth of ~10 nm, corresponding to an ~70-fs Gaussian transform-limited pulse. The spectrum was displayed by a grating polychromator connected to a CCD camera, and the pulse width was measured by the second-harmonic-generation autocorrelation technique.

For the integrated pump–probe measurements the laser beam was split into two parts by a 90/10 beam splitter, and the more intense beam was used to excite the sample while the weaker beam was used as an analyzing light. The excitation and analyzing beams were focused to a common spot of ~50-μm diameter; the probe beam had a slightly smaller size. A maximum pulse energy of 0.8 nJ was used, corresponding to a photon density of $\sim 1 \times 10^{14}$ photons cm^{-2} $pulse^{-1}$. Experiments were also performed at tenfold-lower excitation energy, with no noticeable differences in measured kinetics. To record the kinetics, a step-motor-driven delay line controlled by a PC changes the analyzing pulse's path length. The probe beam intensity was detected by a photodiode and a lock-in amplifier, and as a preliminary characterization the resulting kinetic traces were analyzed in terms of a sum of exponentials by a least-squares fitting procedure including deconvolution with the measured pulse autocorrelation function. A schematic representation of this experimental setup is shown in Fig. 1. As is described below, a more detailed analysis of the measured kinetics was performed by use of a master equation description of the energy transfer in a spectrally inhomogeneous antenna.

To enhance the spectral resolution, two-color measurements were also performed in a dispersed arrangement. For this purpose we used the same experimental setup as in the integrated one-color measurements, but a

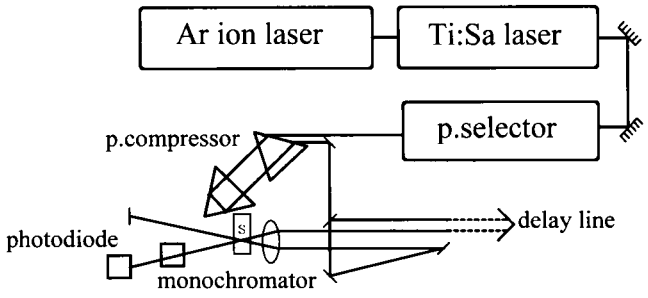

FIGURE 1 Schematic diagram of lasers and optics for a one-color time-resolved absorption experimental setup for the magic angle and anisotropy experiments at room temperature and 77 K.

monochromator with a 1-nm detection bandwidth was placed after the sample. Inasmuch as the spectral filtering is performed after the sample this will not influence the temporal resolution of the experiments, but care has to be exercised with spectral oscillations that may arise in the wings of the pulse spectrum (Chachisvilis et al., 1995a) because of the free induction decay of the polarization induced by the probe pulses.

Femtosecond two-color pump–probe experiments

Two different types of two-color pump–probe arrangement were used: an amplified dye laser and a Ti:sapphire laser pumped optical parametric oscillator (OPO).

Amplified femtosecond dye laser system

This transient absorption spectrometer has been described elsewhere (Åberg et al., 1994), so only a brief account will be given here. We examined the dynamics of Bchl *a* in solution by measuring both the spectral evolution and the transient absorption kinetics at selected wavelengths. For both types of measurement we used a single-jet dye laser synchronously pumped by the compressed and frequency-doubled pulses from a cw Nd:YAG laser (82 MHz, 3 ps, 532 nm, 1.1 W). With an appropriate dye and optics combination this dye laser delivers 250–350-fs tunable pulses in the range 570–700 nm. For the present measurements, R6G was used as the gain medium and the tuning element was a one-plate birefringent filter. This yielded 300-fs pulses (FWHM) at 590 nm with an average power of 250 mW at 82 MHz. The duration of the dye laser pulses was further reduced to 75 fs (75 mW) by a fiber–prism compressor. These pulses were then amplified 10,000-fold in a two-stage dye amplifier pumped longitudinally by a regenerative YAG amplifier working at 1 kHz. Kiton Red in methanol was used as the gain medium in both stages of the amplifier. The amplifier output was ~20 μJ/pulse at 590 nm with 200-fs pulses. The pulses from the amplifier were divided by a 50/50 beam splitter into two parts, one for excitation of the sample and the other generating a white-light continuum to serve as tunable analyzing light from 350 to 900 nm. The continuum light was divided by a 50/50 beam splitter to give an analyzing beam probing the transmission changes of the sample and a reference beam to allow for compensation of intensity fluctuations in the probe light. All three beams, excitation, analyzing, and reference, were focused into the sample with a lens of 100-mm focal length. Only the excitation and analyzing beams were overlapped in space inside the sample, with the excitation beam ~25% larger than the analyzing beam. A monochromator after the sample selected the analyzing (and reference) wavelength, and the excitation beam was blocked. Two photodiodes after the monochromator monitored the analyzing and reference light beams. A chopper was placed in the excitation light so the signal recorded was $\log(I/I_{ref})_{w.o.ex.} - \log(I/I_{ref})_{w.ex.}$. In this way each analyzing pulse was individually detected and normalized. The excitation pulse energy was also measured, and only data obtained with pulses within a preset intensity range were accepted.

Transient absorption kinetics at a particular probe wavelength were measured by stepping the optical delay line in the excitation beam path, for a fixed setting of the probe monochromator. In measuring time-resolved difference absorption (ΔA) spectra care has to be taken to avoid errors from the wavelength chirp that are due to group-velocity dispersion in the continuum. This gives a wavelength dependence of time 0 when different parts of the continuum arrive at the sample at different times. To correct for the effect, the delay in the excitation beam was moved according to a preset calibration while a spectrum was recorded. The calibration of the dispersion was made by measuring time 0 in different dye solutions and two-photon absorption in diphenyl hexatriene at different wavelengths. The result was fitted to an analytical expression that was used to move the delay line. The accuracy of zero time is estimated to be within 100 fs over the spectral range used in the present measurements, and the time resolution of the kinetic measurements (analyzed by least-squares fitting a sum of exponentials convoluted with the apparatus response function) is approximately 200 fs.

Ti:sapphire optical parametric oscillator femtosecond system

To examine directly the transfer of excitation energy from B800 to B850 in *Rb. sphaeroides* free from exciton annihilation, low-energy femtosecond Ti:sapphire pulses were used. The excitation and independently tunable probe pulses were generated with a synchronously pumped OPO. When this OPO was pumped by the 82-MHz pulse train of the Ti: sapphire laser, it generated two new output wavelengths, the signal (~300 mW) and the slightly less powerful idler (~ 200 mW). The total wavelength coverage of the OPO is from 1.1 to 2.6 μm, and with ~80-fs pump pulses cross-correlation pulses with the pump of ~100 and ~130 fs were measured for the signal and the idler pulses, respectively. The good synchronization among the pump, signal, and idler pulses with this system permits the measurement of femtosecond pump–probe absorption kinetics.

To measure the direct energy transfer from B800 to B850 we excited the sample at ~807 nm by using the residual pump light reflected from the front surface of the LBO crystal in the OPO (see Fig. 2). Probe pulses tunable over the range 830–875 nm were generated by frequency doubling the idler pulses in a BBO crystal. The 1-mm path length of the crystal caused a broadening of the apparatus response function to ~190 fs.

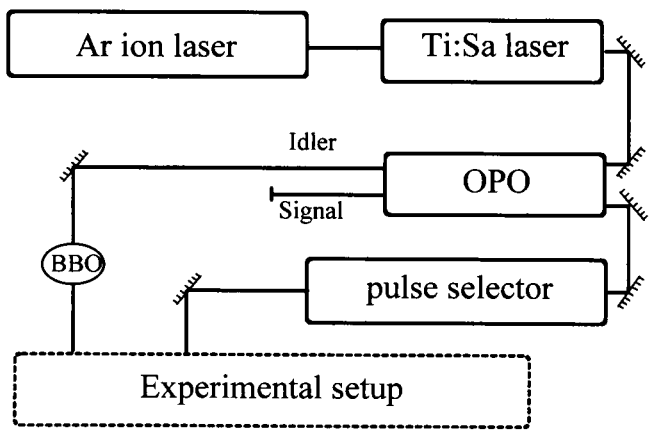

FIGURE 2 Experimental arrangement used for direct observation of the B800→B850 energy transfer in the LH2 antenna complex of *Rb.sphaeroides* WT at room temperature, based on a femtosecond OPO pumped by a mode-locked Ti:sapphire laser.

Sample treatment

The energy-transfer properties were measured in intact chromatophores of *Rb. sphaeroides* and *Rps. palustris* LL at room temperature and at 77 K. Preparation of the chromatophores was described in detail previously (Sundström et al., 1986; Bergström et al., 1986). Briefly, the chromatophores were prepared from cells by sonication and diluted in 50-mM TRIS buffer solution at pH 8.0 to yield a solution of the desired optical density, ~0.6. Room-temperature measurements were performed with the sample in a spinning cell, and for the 77-K measurements a liquid-nitrogen cryostat (Oxford Instruments Ltd., Oxford, UK) was used, with the sample in a stationary 1-mm cell. To obtain a glass of good optical quality we mixed the membrane suspensions with glycerol (70% glycerol and 30% preparation). The excited-state dynamics of Bchl *a* were measured in alcohol solutions; for these measurements a 1-mm flow cell was used at room temperature to reduce photodegradation of the sample, and the measurements at 77 K were performed in a 1-mm stationary cell cooled by an Oxford Instruments liquid-nitrogen cryostat. Spectroscopic-grade solvents were used in all measurements.

Bchl *a* IN SOLUTION AND IN LOW-TEMPERATURE GLASSES

Earlier studies of energy transfer in B800 revealed a fast subpicosecond decay component of the B800 excited state (~300 fs at room temperature) that appeared to have no corresponding lifetime in the anisotropy decays (Hess et al., 1993). It was suggested that this fast component could be due to some internal relaxation within Bchl *a*, such as vibrational relaxation and cooling instead of energy transfer within B800. From time-resolved measurements of dye molecules it is known that processes such as solvation (Maroncelli et al., 1989), vibrational relaxation (Elsaesser and Kaiser, 1991), and conformational changes and dissipation of excess vibrational energy (Åberg et al., 1994) may give rise to subpicosecond and picosecond transients in time-resolved fluorescence and ground-state absorption measurements. In this study we are interested in determining whether such fast relaxation processes exist in the Bchl *a* molecule and whether they could obscure the results from studies of energy transfer in purple bacteria. To discriminate the intramolecular relaxation processes from those associated with energy transfer we performed measurements on Bchl *a* in solution, in the absence of energy transfer.

In this study the Q_x band was excited with 590-nm ~200 fs pulses and difference absorption kinetics and spectra were measured in the wavelength region of the Q_y absorption and fluorescence bands of Bchl *a*. From the kinetic measurements we can see that there exist relaxation processes that are far faster than the decay of the excited state on a nanosecond time scale. In Fig. 3, three kinetic traces of Bchl *a* in methanol at different analyzing wavelengths are presented. At the blue side of the Q_y absorption maximum (740 nm) we can see an initial bleach that is rapidly relaxing to a constant level. This relaxation is best characterized by two lifetimes, ~1 and ~10 ps. If the analyzing wavelength is shifted toward the red within the Q_y band, the amplitudes of the fast decays are reduced, and kinetics with rise times similar to the decay times at the shorter wavelengths are observed at probe wavelengths longer than approximately

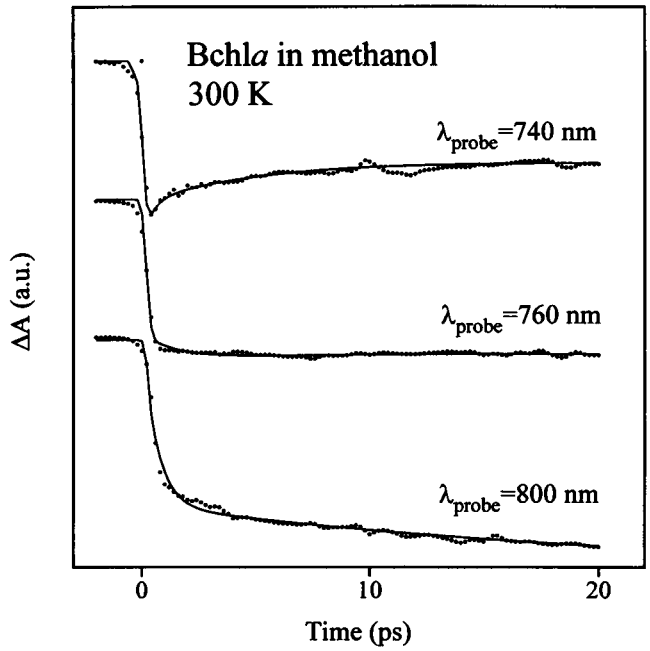

FIGURE 3 Two-color transient absorption measurements of Bchl *a* in methanol at room temperature. The experiments were performed by exciting at 590 nm and probing at 740, 760, and 800 nm. The kinetics were fitted to a sum of three exponentials, giving T_1 = 1.1 ps (A_1 = −1.35), T_2 = 8.1 ps (A_2 = −1.52), and $T_3 \geq$ 100 ps (A_3 = −5.0) at 740 nm; T_1 = 1.2 ps (A_1 = 0.2), T_2 = 17.2 ps (A_2 = 0.9), and $T_3 \geq$ 100 ps (A_3 = −1.20) at 760 nm; and T_1 = 1.6 ps (A_1 = 0.2), T_2 = 18.1 ps (A_2 = 0.5), and $T_3 \geq$ 100 ps (A_3 = −1.23) at 800 nm.

the ground-state absorption maximum (kinetic traces at 760 and 800 nm of Fig. 3).

The origin of the kinetics becomes clearer from the transient absorption difference spectra of Fig. 4. A spectral

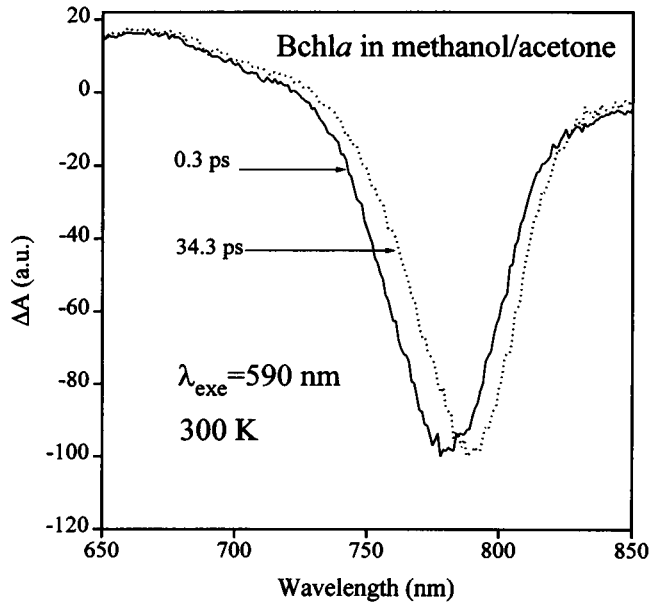

FIGURE 4 Transient absorption spectra of Bchl *a* in a methanol/acetone solution at room temperature after excitation at 590 nm.

evolution occurs on a femtosecond–picosecond time scale, implying a narrowing and a red shift of the spectrum. The measured transient spectrum is a compound result of ground-state bleaching (~770 nm), stimulated emission (~780 nm), and excited-state absorption (<725 nm). Observed spectral shifts and kinetic transients will consequently be a measure of relaxation processes within both the excited and the ground electronic states. Solvation of the excited molecule is known to produce spectral shifts of the fluorescence (stimulated emission) and excited-state absorption spectra, whereas vibrational relaxation/cooling is expected to produce mainly a spectral narrowing (Elsaesser and Kaiser, 1991; Savikhin and Struve, 1994) and fewer spectral shifts owing to the weak electron–phonon coupling in Bchl *a* (Reddy et al., 1991). When the maximum of the bleached band is plotted versus time, (Fig. 5), a fast spectral red shift on two time scales, ~0.7 ps (A = 64%) and ~10–20 ps (A = 36%), is observed for Bchl *a* in a methanol/acetone mixture. For Bchl *a* in butanol the observations are similar, but the fast component is approximately a factor of 2 slower (1.3 ps), and there is a higher amplitude of the slower component (A = 57%).

One usually measures polar solvation times by using various dye molecules. The solvation time is characteristic of the polar solvent and ideally is independent of the probe molecule. Solvation dynamics in alcohols is generally characterized by nonexponential kinetics; for methanol two lifetimes, $T_1 \approx 1$ ps and $T_2 \approx 10$ ps, have been obtained, and for butanol the corresponding lifetimes are $T_1 \approx 20$ ps and $T_2 \approx 100$ ps (Castner et al., 1987; Weaver et al., 1990). This suggests that the ~1- and 10–20-ps relaxation processes observed in our measurements of Bchl *a* in solution at room temperature may originate from spectral changes that are related to the solvation of the Bchl *a* excited state.

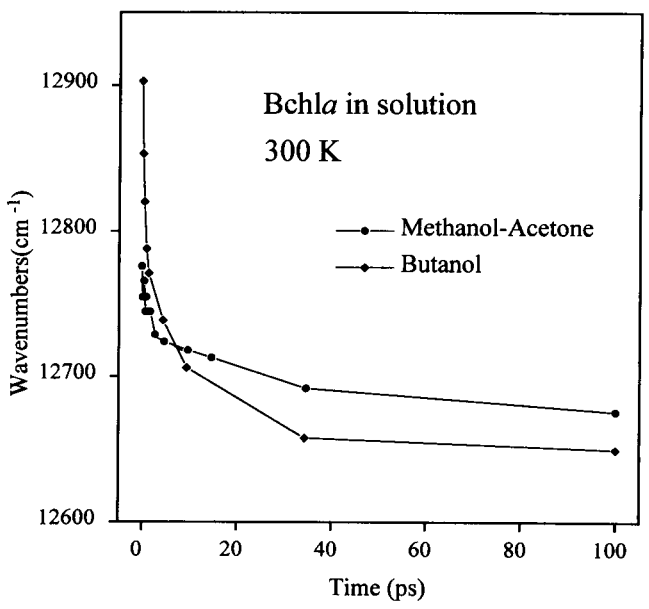

FIGURE 5 Time dependence of the position of the maximum of the bleached band of Bchl *a* in two different solvents, methanol/acetone and butanol, at room temperature. The decays were fitted by a sum of two exponentials, resulting the following lifetimes: T_1 = ~0.7 ± 0.3 ps (A_1 = 65 ± 5%) and T_2 = 10–20 ps (A_2 = 35 ± 5%) for the methanol/acetone mixture and T_1 = ~1.3 ± 0.3 ps (A_1 = 45 ± 5%) and T_2 = 10–20 ps (A_2 = 55 ± 5%) for butanol.

In our experiments we excite the Q_x electronic transition of Bchl *a* with 590-nm laser light. This produces a large excess vibrational energy when the molecule relaxes to the Q_y state. The vibrational relaxation following the $Q_x \rightarrow Q_y$ transition and cooling of the resulting nonequilibrium vibrational distribution may give rise to spectral shifts on time scales of subpicoseconds to tens of picoseconds (Elsaesser and Kaiser, 1991). In an attempt to distinguish between solvation and vibrational relaxation/cooling we measured the picosecond dynamics of Bchl *a* in a frozen solvent, ethanol at 77 K. In principle, our kinetic measurements should also contain a kinetic component corresponding to the $S_2 \rightarrow S_1$ internal conversion process. This relaxation is fast, and from recent measurements of bacterial reaction centers (Du et al, 1992; Jia et al., 1995) it appears likely that it is characterized by an ~150-fs time constant. Considering the present time resolution of ~200 fs and the already complex kinetics that result from solvation and vibrational relaxation/cooling, we did not attempt to resolve this relaxation process separately in our measured kinetics; it is included in the fast 0.5–1-ps component that we observe. At 77 K ethanol forms a glass, so the contribution of solvent relaxation to the spectral changes is minimized on the picosecond time scale. Bchl *a* is sensitive to light and tends to photodegrade, as mentioned earlier. Therefore, in the low-temperature measurements care was taken to use as low light intensities as possible, and the sample was translated perpendicular to the beam while the measurement was made. We performed measurements with different excitation energies by placing neutral-density filters in the path of the excitation beam. Because of the photosensitivity of the sample it was not possible to measure the spectral evolution directly, as measurements of transient spectra require very stable absorption spectra (i.e., no slow changes resulting from degradation) over quite a long measuring time. From the room-temperature measurements we know that the effect of the spectral change is most pronounced on the blue side of the bleaching maximum, so if spectral shifts or narrowing is present at 77 K we expect it to be most easily revealed in a kinetic measurement near 740–750 nm. As can be seen from the kinetics in Fig. 6, there is some relatively slow relaxation with a 10 ± 3-ps time constant in this wavelength region. These results suggest that there exist vibrational relaxation and cooling processes on a time scale similar to that of the slower parts of the solvation dynamics, i.e., ~10 ps. But the faster ~1 ps component observed at room temperature appears now to be absent. Relaxation processes on a time scale of ~10 ps observed by spectral hole burning at a very low temperature (Avarmaa and Rebane, 1985) were interpreted in a similar way. We notice that these processes are considerably slower than the energy-transfer processes of interest here. It has to be mentioned

that the kinetics of Bchl *a* were measured with ~200-fs pulses, which implies that processes substantially faster than 0.5–1.0 ps may be difficult to detect. Thus, if very fast (~100 fs or faster) relaxation processes exist in Bchl *a* they may have escaped detection in the present experiments.

In *Rb. sphaeroides* and *Rps. palustris* the subpicosecond component in the B800 excited-state decay shows very little temperature dependence, increasing only from ~200 fs to ~300 fs when the temperature is decreased from room temperature to 77 K and the relative amplitude increases (see the following section). In addition, this component measured at the magic angle is correlated to a similar decay of anisotropy (see below). These characteristics of the B800 excited-state dynamics, when compared with the Bchl *a*/solution and Bchl *a*/low-temperature glass dynamics described above, strongly suggest that the kinetics and transient spectral evolution of B800 on subpicosecond and few-picosecond time scales are largely dominated by energy transfer and that intramolecular relaxation processes play only a minor role. Here it should also be pointed out that the measurements of Bchl *a* in solution and in low-temperature glasses were performed with Q_x excitation, whereas the measurements on LH2 were performed with Q_y excitation. Q_x excitation will generate more excess vibrational energy, which could cause some differences in the vibrational relaxation/cooling of the Bchl *a* molecule. However, the similarity of the observed time constants in the present work and in that of Savikhin and Struve (1994) (Q_y excitation) and Becker et al. (1990; 1991) (Q_x excitation) suggests that the relaxation dynamics with the two modes of excitation in fact are quite similar, at least on the subpicosecond–picosecond time scale.

Both Becker et al. (1990, 1991) and Savikhin and Struve (1994) found a fast ~1-ps relaxation time in addition to slower components on the ~10-~100-ps time scale in their room-temperature kinetic measurements of Bchl *a* in solution. Becker et al. (1990, 1991) concluded that the slower relaxation is due to solvent relaxation, whereas the origin of the faster relaxation remained unclear. Savikhin and Struve (1994) considered vibrational cooling/intermolecular vibrational energy redistribution and dielectric relaxation as possible mechanisms for the observed relaxations, and they discussed various dynamic "scenarios" that could occur, depending on the time scales on which the various processes take place. From the comparison with the experimental results they could conclude that vibrational equilibration/intermolecular vibrational redistribution was a major contributor to the observed femtosecond and picosecond kinetics of Bchl *a* in 1−propanol at room temperature. Dielectric relaxation was also considered to be present, but from their data alone they could not assign a time scale to these processes in Bchl *a*. However, from our measurements of the Bchl *a* relaxation in alcohol solutions and low-temperature glasses it is possible to conclude that solvation is perhaps mainly responsible for the fastest processes whereas cooling and excess energy dissipation in addition contribute to the slower process on the tens-of-picoseconds time scale.

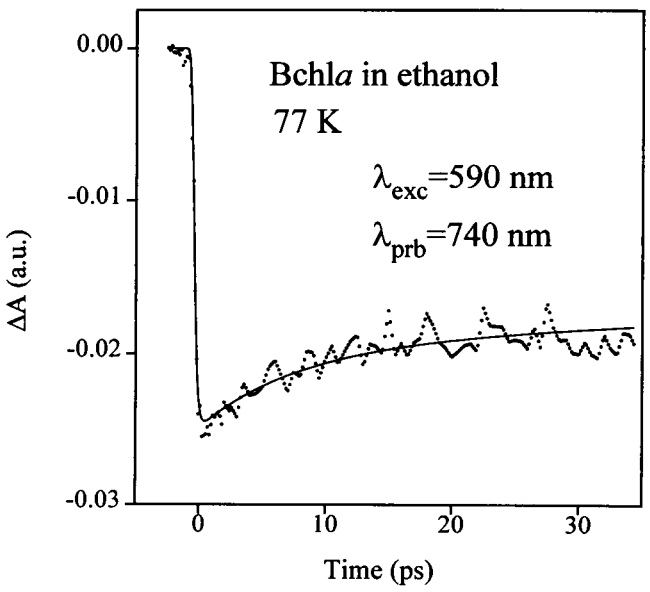

FIGURE 6 Kinetics of Bchl *a* in ethanol at 77 K. The samples were excited at 590 nm and probed at 740 nm. The best fit gave the following lifetimes: T_1 = 11 ± 4 ps (A_1 = 30 ± 10%) and $T_2 \geq$ 100 ps (A_2 = 70%).

B800 TO B850 ENERGY TRANSFER

Fig. 7 displays kinetics of LH2 in *Rb. sphaeroides* at room temperature monitored in the B800 band (Fig. 7 *A*) and at several wavelengths within the B850 band (Fig. 7 *B*) after excitation of B800. Probing the kinetics at ~800 nm (Fig. 7 *A*) monitors the decay of the B800 excited state, and, in agreement with earlier room-temperature measurements (Hess et al., 1993), we found it to be characterized by a 0.7 ± 0.05-ps time constant as well as a faster ~0.3-ps component, with relative amplitudes similar to those reported earlier; the bigger amplitude of the fast component obtained here compared with that in the earlier work of Hess et al. (1993) is most likely a result of the better time resolution of the present measurements. The 0.7 ± 0.05-ps decay phase of B800* is matched by the corresponding rise time of the B850 excited-state bleaching as monitored at 875 nm in the red wing of B850. In combination with the results in the previous section this demonstrates that the transfer of energy from B800 to B850 occurs with a time constant of 0.7 ± 0.05 ps at room temperature and that additional faster decay components monitored in the 800-nm band are due to energy transfer within B800. In the kinetic trace of Fig. 7 *B* measured at 840-nm probe wavelength there is an initial very fast ~150-fs rise of the bleaching signal followed by a decay characterized by the same ~0.7-ps time constant as observed in the red wing of the 850-nm band. The ~150-fs component is also observed as a rise time of the other probe wavelengths (850–875 nm), with the maximum relative amplitude in the kinetic curve measured at 850 nm, close to the isoasbestic wavelength of the slower components. This

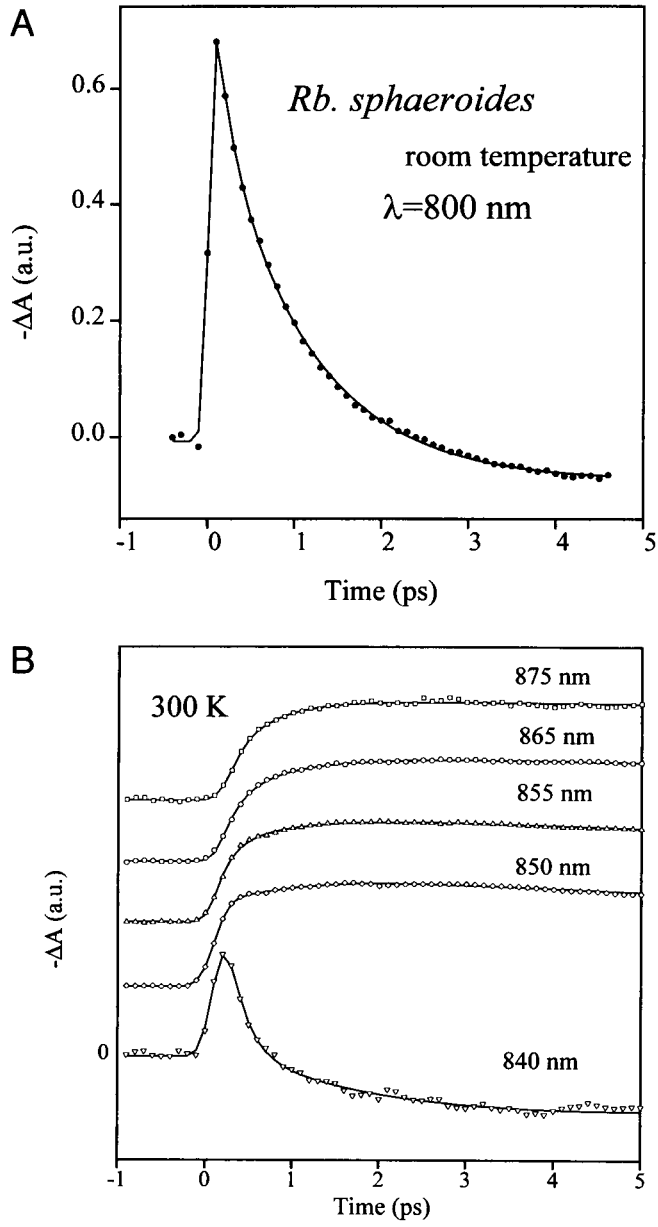

FIGURE 7 A. Magic angle integrated one-color absorption recovery of *Rb. sphaeroides* WT, measured at 800 nm at room temperature. The solid curve represents the three-exponential fit with the following lifetimes and amplitudes: T_1 = 200 ± 50 fs (A_1 = 1.0), T_2 = 0.7 ± 0.05 ps (A_2 = 0.6), and $T_3 \geq 30$ ps (A_3 = −0.1). B. Transient absorption kinetics of LH2 *Rb. sphaeroides* WT excited into the B800 band and probed at different wavelengths within the B850 band at room temperature. The solid curves are the best fits with the following lifetimes at different wavelengths: at 840 nm, T_1 = 150 fs (A_1 = −0.3) and T_2 = 0.70 ps (A_2 = 1.41); at 850 nm, T_1 = 130 fs (A_1 = −0.3) and T_2 = 0.65 ps (A_2 = −0.28); at 855 nm, T_1 = 130 fs (A_1 = −0.3) and T_2 = 0.64 ps (A_2 = −0.35); at 865 nm, T_1 = 150 fs (A_1 = −0.3) and T_2 = 0.66 ps (A_2 = −0.51); and at 875 nm, T_1 = 170 fs (A_1 = −0.3) and T_2 = 0.69 ps (A_2 = −0.58).

behavior is a result of very fast 100–200-fs energy equilibration within B850 and could be due either to a Förster type of incoherent energy transfer among spectrally nonequivalent (spectral inhomogeneity) B850 molecules or to relaxation in the strongly coupled B850 pigments. At the moment it is not clear which of these descriptions is more relevant to B850. This effect is analyzed more thoroughly in a subsequent paper (Hess et al., in press).

At 77 K we monitored the B800→B850 energy transfer in *Rb. sphaeroides* and *Rps. palustris* by probing the decay of the B800 excited state with spectrally integrated probing at different wavelengths within the B800 band. Magic angle kinetics of *Rb. sphaeroides* at three different wavelengths, 790, 800, and 810 nm, are shown in Fig. 8A. Lifetimes and amplitudes obtained from both *Rb. sphaeroides* and *Rps. palustris* are collected in Table 1. The decay of the bleaching is, as at room temperature (see Fig. 7 *A*), clearly nonexponential at all wavelengths but is slower than at room temperature. The relaxation time corresponding to B800→B850 energy transfer has increased from ~0.7 to ~1.8 ps, whereas the faster subpicosecond lifetime has become only slightly longer, increased from 0.3 to ~0.4 ps. The negative induced absorption signal is characterized by a much slower decay time constant, >30 ps, which from previous picosecond studies (Zhang et al., 1992) is known to represent the energy equilibration between the different antenna systems (LH2 and LH1) and quenching by the closed reaction centers.

In a complementary set of measurements of the B800* lifetime at 77 K we used a monochromator after the sample to select a narrow spectral region of the signal. Although spectrally broadband excitation is used also in these experiments, the narrow detection bandwidth results in better spectral resolution of the dynamics. The 77-K results of the B800 excited-state decay probed with integrated and dispersed probe light in the 800-nm band are summarized in Tables 1 and 2, respectively. As can be seen, both detection methods yield very similar lifetimes and wavelength variation of the amplitudes, A_i. These results show that the energy transfer from B800 to B850 at 77 K is similar in *Rb. sphaeroides* and *Rps. palustris* (~1.8 ± 0.2 ps), which is reasonable in view of the expected structural similarity of the two complexes (Van Mourik et al., 1992). The lengthening of the transfer time from ~0.7 ps at room temperature to ~1.8 ps at 77 K is a result of decreased spectral overlap at low temperature and has been discussed previously (Bergström et al., 1988). The time constant for B800→B850 energy transfer at 77 K (1.8 ± 0.2 ps) found here is somewhat shorter than the 2.4 ps reported previously (Hess et al., 1994). The main reason for this difference lies in the basic difficulties of fitting multiexponential decay curves (James and Ware, 1985). The present data cover several wavelengths, including both one- and two-color measurements. In that way various decay components could be better resolved. Comparison of the present results and hole-burning results obtained at ~4 K shows that the B800→B850 transfer time slows down somewhat more below 77 K, which is in agreement with recent simulations of the energy-transfer process (Hess et al., 1994). The simulation results verified and substantiated a pre-

vious suggestion by Reddy et al. (1991) that, at low temperature, overlap between the B800 fluorescence and a vibrational feature of B850 is essential in accounting for the observed energy-transfer rate.

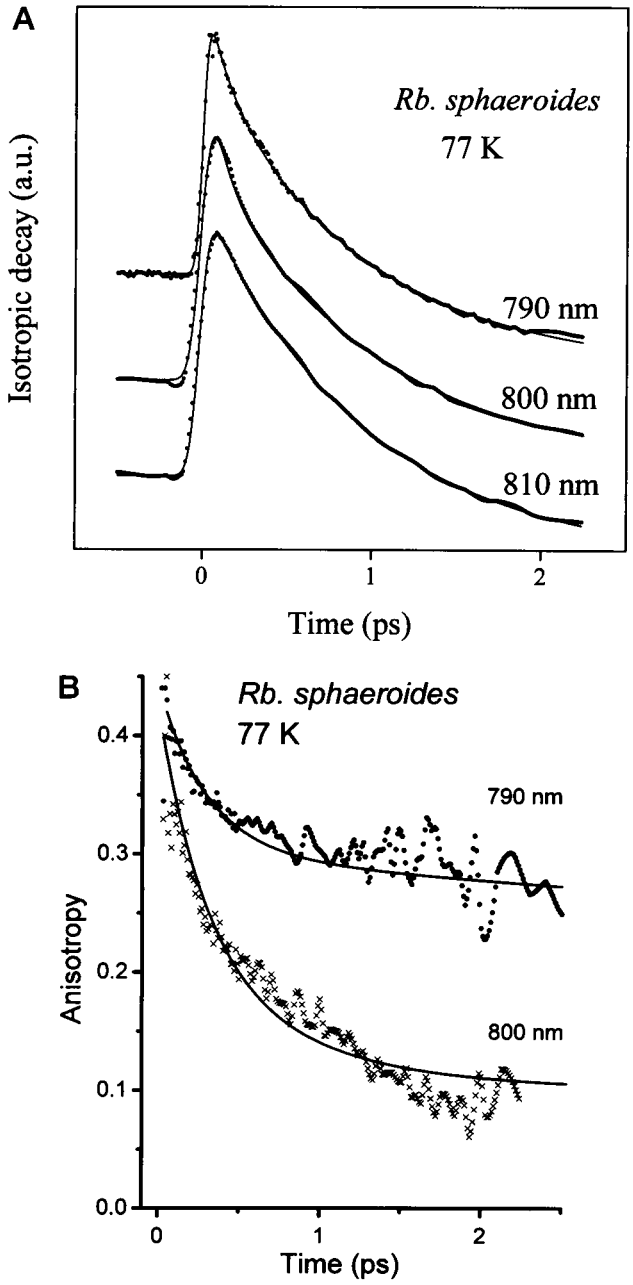

FIGURE 8 A. Magic angle absorption recovery kinetics of the B800 band of *Rb. sphaeroides*, measured at three different wavelengths (790, 800, and 810 nm) at 77K. The corresponding lifetimes and amplitudes are presented in Table 1. B. Anisotropy decay obtained from parallel and perpendicular kinetics of *Rb. sphaeroides* at 77K at two wavelengths (790 and 800 nm). The solid curves represent the best fits with the following parameters: at 790 nm, T_1 = 0.3 ± 0.1 ps (A_1 = 0.12), T_2 = 5 ± 1.5 ps (A_2 = 0.08), $r(\infty)$ = 0.2; at 800 nm, T_1 = 0.3 ± 0.1 ps (A_1 = 0.2), T_2 = 1.5±.5 ps (A_2 = 0.1), $r(\infty)$ = 0.1.

TABLE 1 B800* lifetimes at various wavelengths within the B800 absorption band for *Rb. sphaeroides* and *Rps. palustris* at 77 K

λ (nm)	T_1 (ps)	A_1	T_2 (ps)	A_2	T_3 (ps)	A_3
*Rb. sphaeroides**						
790	0.33	1	1.67	0.60	>30	−0.25
800	0.46	1	1.80	0.62	>30	−0.31
810	0.60	1	1.90	0.64	>30	−0.48
Rps. palustris‡						
790	0.24	1	1.65	0.73	>30	−0.28
800	0.32	1	1.76	0.82	>30	−0.39
810	0.44	1	1.98	0.86	>30	−0.50

The results were obtained with integrate absorption pump-probe detection technique.
*The standard errors are 15% for T_1, 10% for T_2, and 20% for T_3.
‡The variations of the lifetimes are 20%, 10%, and 30% for T_1, T_2, and T_3, respectively.

RELAXATION DYNAMICS WITHIN B800

Having established above that energy transfer from B800 to B850 occurs with a time constant of ~0.7 ps at room temperature and ~1.8 ps at 77 K, we now proceed with the dynamics related to processes within B800. The relaxation in B800 may be either intramolecular (vibronic relaxation, e.g.) or intermolecular (excitation transfer). First we note that the absence of subpicosecond processes in the excited-state decay of Bchl *a* in solution at 77 K suggests that the ~0.5-ps decay component observed in *Rb. sphaeroides* and *Rps. palustris* at 77 K originates mainly from energy transfer within B800. As molecules in B800 are not identical (different orientation of transition dipole moments, spectral inhomogeneity), the energy transfer can be monitored in two different ways. Excitation transfer between molecules of different energy (spectral equilibration) is resolved in isotropic measurements, and the energy transfer between differently oriented chromophores can be monitored by time-resolved anisotropy (Sundström et al., 1986) measurements. The relationship between these two observables yields complementary information about the dynamics and can be used to deduce information about the degree of order in the system. In the next section we show how a master equation model is used to simulate these processes.

Earlier picosecond measurements at 77 K within the B800 band of *Rb. sphaeroides* (Van Grondelle et al., 1987) indicated that the anisotropy of the B800 excited state remained quite high throughout its lifetime, suggesting only limited energy transfer or energy transfer between close-to-parallel B800 transition dipoles. However, with picosecond resolution it was not possible to resolve any details of the time dependence of the B800 anisotropy. More recent measurements with ~100 fs-pulses on *Rb. sphaeroides* and *Rps. palustris* (Hess et al., 1993) revealed that at room temperature there is a 0.8–1.5-ps decay of the B800 anisotropy. The fact that the anisotropy decay is slower than the isotropic B800 excited-state decay explains the difficulties in resolution of this decay in earlier experiments with lower time resolution.

The results of the present measurements of *Rb. sphaeroides* at 77 K are illustrated by the polarized kinetics and calculated anisotropy decays of Figs. 8 *A* and *B*, respectively. Qualitatively similar results are obtained for both species at all studied wavelengths within the B800 band. The anisotropy starts very close to the theoretical maximum value of 0.4 and decays with a time constant of 0.3 ps to a lower value $r(\infty) = \sim 0.15$–0.30. Besides the fast component there is also a slower ($\geq$1-ps) decay. The value of the long-time anisotropy $r(\infty)$ is wavelength dependent; in the center of the absorption band at ~800 nm it assumes a relatively low value ($r(\infty) = \sim 0.1$), whereas in the blue wing of the B800 absorption band it is considerably higher, $r(\infty) = 0.2$–0.25. This suggests that there is more efficient excitation transfer among the B800 pigment molecules absorbing at the center of the absorption band than among with those absorbing in the wings of the spectrum. In the following section we show that this behavior is a result of the inhomogeneous spectral broadening of B800 and relatively narrow homogeneous spectral width at low temperature, which result in trapping of excitations in both wings of the inhomogeneous distribution function (IDF).

To obtain the anisotropy decay from the measured traces with parallel and perpendicular probe polarizations, it is necessary to subtract the negative signal contribution from the B850 excited-state absorption. This was done by simulating the rise of this signal with the rate of B800→B850 energy transfer as obtained from the magic angle measurements of the B800* decay (Tables 1 and 2) (Hess et al., 1993) and assuming that the B850 signal is depolarized after the B800→B850 transfer. This appears as a reasonable approximation considering the pigment organization of LH2 (McDermott et al., 1995) and the fact that B850 depolarization (measured with direct B850 excitation (Chachisvilis et al. 1995b) is much faster ($\leq$200 fs) than the B800 excited-state decay. The amplitude of the isotropic ~150-fs component assigned to energy equilibration within B850 is in addition very low at these wavelengths, far away from the isosbestic wavelength of B850 bleaching.

We saw above that the isotropic decay of the B800 excited state (Tables 1 and 2; Fig. 8 *A*) is characterized by an ~0.4-ps time constant at 77 K (~0.3 ps at room temperature) in addition to the ~1.8 ± 0.2-ps time for B800→B850 transfer (~0.7 ps at room temperature). The similar anisotropy and magic angle decay times along with the fact that the B800 spectrum is largely characterized by inhomogeneous broadening strongly suggest that the ~0.4-ps isotropic decay time is a result of energy transfer within B800 rather than of, e.g., vibrational relaxation/cooling.

As can be seen from Fig. 8 *A*, we measured the isotropic decay of B800 in the red wing of the absorption band at ~810 nm. To measure the anisotropy decay accurately at the same wavelength turned out to be more difficult, and we could not obtain a reliable decay with quality comparable with that obtained at 790 and 800 nm. The reason for this problem is that at this wavelength there is very low absorption from B800 and the amplitude of B850 excited-state absorption is higher. This results in a very fast change of sign of the parallel and perpendicular signals. We have developed a way to correct our data for the negative signal that is due to the excited-state absorption (Hess et al., 1993), but it can result in quite a big error if the excited-state absorption is too intense. Furthermore, at this wavelength the B850 is already directly excited to some extent, which makes the correction even more problematic. From the experimental data in this part of the spectrum we can therefore conclude only that the anisotropy is relatively high at all times ($\geq$0.2), but no reliable value of an initial decay phase can be ascertained. However, despite all these problems, what we see is qualitatively in agreement with simulations (see the following section).

SIMULATIONS

Master equation and spectral overlap

We describe excitation transfer in B800 as incoherent hopping in a two-dimensional spectrally inhomogeneous antenna lattice. Adopting the model of Pullerits and Freiberg (1992), we write down the Pauli master equation, which describes the kinetics of this process, in matrix form as

$$\mathbf{P}(t) = \mathbf{R} * \mathbf{P}(0). \quad (1)$$

The rate matrix R contains information about the pairwise transfer rates and the loss channels. Here the dominating loss channel is the transfer B800→B850. Corresponding backtransfer at 77 K as well as other possible loss channels (spontaneous emission, internal conversion, intersystem crossing) may be considered insignificant in our case.

The Green function approach to the solution of the master equation gives us relatively simple formulas to calculate both isotropic and polarized experimental signals if the necessary spectral (inhomogeneous distribution, homogeneous spectra) and orientational (orientation of the transition dipole moments of the molecules) information of the system is provided. The formalism and derivations can be found in Pullerits and Freiberg (1992) and Pullerits et al. (1994c), and we will not repeat them here.

According to the Förster theory (Förster, 1965), the incoherent excitation transfer rate is proportional to the overlap integral of the emission spectrum of the donor $f_D(\nu)$ and

TABLE 2 B800* lifetimes for *Rb. sphaeroides* obtained with the dispersed absorption pump-probe detection technique and measured at 77 K

λ (nm)	T_1 (ps)	A_1	T_2 (ps)	A_2	T_3 (ps)	A_3
790	0.33	1	2.0	0.4	>30	−0.6
800	0.36	1	1.86	0.6	>30	−0.4
810	0.39	1	1.63	0.7	>30	−0.2

The given values are averages of five independent measurements with a standard deviation of ~20%.

the absorption spectrum of the acceptor $\epsilon_A(\nu)$:

$$k_{et} = C\kappa^2 \int f_D(\nu)\epsilon_A(\nu)\, d\nu, \qquad (2)$$

where C does not depend on the energy (strictly speaking C is not independent of ν, but we ignore this weak dependence in our qualitative calculations) and κ^2 is the factor that depends on the mutual orientation of the two transition dipole moments. Because of the short excited-state lifetime of B800 the fluorescence spectrum $f_D(\nu)$ is not very accurately measurable. Furthermore, it would not be correct to use directly measured spectra because of the inhomogeneous broadening; in Eq. 2 the homogeneous spectra must be used. Therefore we have carried out spectral simulations of the B800 band of the B800–850 complex, using the model developed by Pullerits et al.(1994b). This model uses the linear harmonic Franck–Condon approximation and permits the calculation of the spectrum of the electronic transition that is coupled to vibronic modes and lattice phonons. We have made use of the vibronic frequencies and relative transition intensities of Bchl *a* reported by Renge et al. (1987). This work does not give values for the Franck–Condon factors, and we have varied these parameters within reasonable limits to get the fit to experimental spectra. To compare the model spectra with experiment, the calculated homogeneous spectra were convoluted with the IDF. The width of the IDF of B800 is taken to be 170 cm^{-1} (Reddy et al., 1991). The experimental and calculated absorption spectra of the B800 band at 150 K and at room temperature are given in the upper panel of Fig. 9. In the calculations of the overlap integral we have assumed that the homogeneous absorption and fluorescence spectra are mirror symmetric with respect to the 0–0 transition frequency.

It has been discussed by Kenkre (1982) that sharp peaks in the homogeneous spectra correspond to slow decay of memory functions in the generalized master equation description and thus indicate the presence of coherent transfer. This is not surprising because in general the same mechanism broadens zero-phonon lines (ZPLs) and randomizes phase of excitations. At 0 K it is quite obvious that the overlap of donor fluorescence with the ZPL of the acceptor absorption does not correspond to incoherent Förster transfer because one of the main assumptions of the Förster theory is not satisfied in that case: there is no fast relaxation from the initially created acceptor state because from the zero-phonon level there is nowhere to relax at low temperature. Thus we have left the ZPL of the acceptor spectrum out of the spectral overlap calculation. Fig. 9 shows the dependence of the spectral overlap on the energy difference between donor and acceptor at 4, 77, and 300 K. IDF is also presented in both panels. The curves of the spectral overlap give the relative transfer rate from the molecule with ZPL at energy $\nu_0 + \Delta E$ to the molecule with the ZPL at the center of the IDF (ν_0). At 4 K the spectral overlap has a structure corresponding to the vibronic bands of the homogeneous spectra. The structure disappears at higher temperature. At

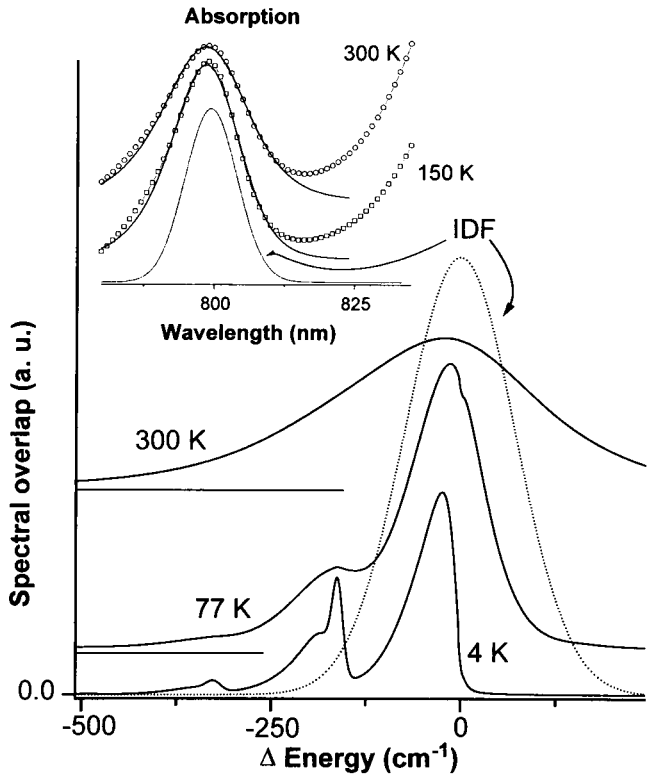

FIGURE 9 Dependence of the calculated Förster spectral overlap on the energy gap between the excitation donor and acceptor at three different temperatures. The overlap of the donor fluorescence with the ZPL of the acceptor is left out of the calculation (see text). Homogeneous absorption and fluorescence spectra are assumed to be mirror symmetric with respect to the ZPL position. The electronic transition is coupled to the protein phonons of mean frequency 20 cm^{-1}, $S = 0.4$, and to an intramolecular vibrational mode of 165 cm^{-1}, $S = 0.1$. The upper panel shows a comparison of experimental and calculated absorption spectra of B800 at two temperatures. For comparison the inhomogeneous distribution function (IDF) of 170 cm^{-1} is also presented in both panels.

77 K and lower the overlap is relatively narrow compared with the IDF, and it can be seen that the transfer rate from the bluest side of IDF to the center of IDF is relatively small.

Model calculations

As a first example we have performed calculations for a two-dimensional hexagonal system of 19 molecules. The transition dipole moments of the molecules are random in the plane, and the energies of the 0–0 electronic transitions are distributed according to the Gaussian IDF of 170 cm^{-1} half-width. In the calculations we also take into account the spectral width of the excitation pulse of 150 cm^{-1}. We have calculated the kinetics of the isotropic and anisotropic pump–probe signals at three different wavelengths, 790, 800, and 810 nm, which correspond to the blue edge, the center, and the red edge of the absorption band, respectively. In Fig. 10 we present the calculated distributions of the decay constants of isotropic kinetics of B800 at these

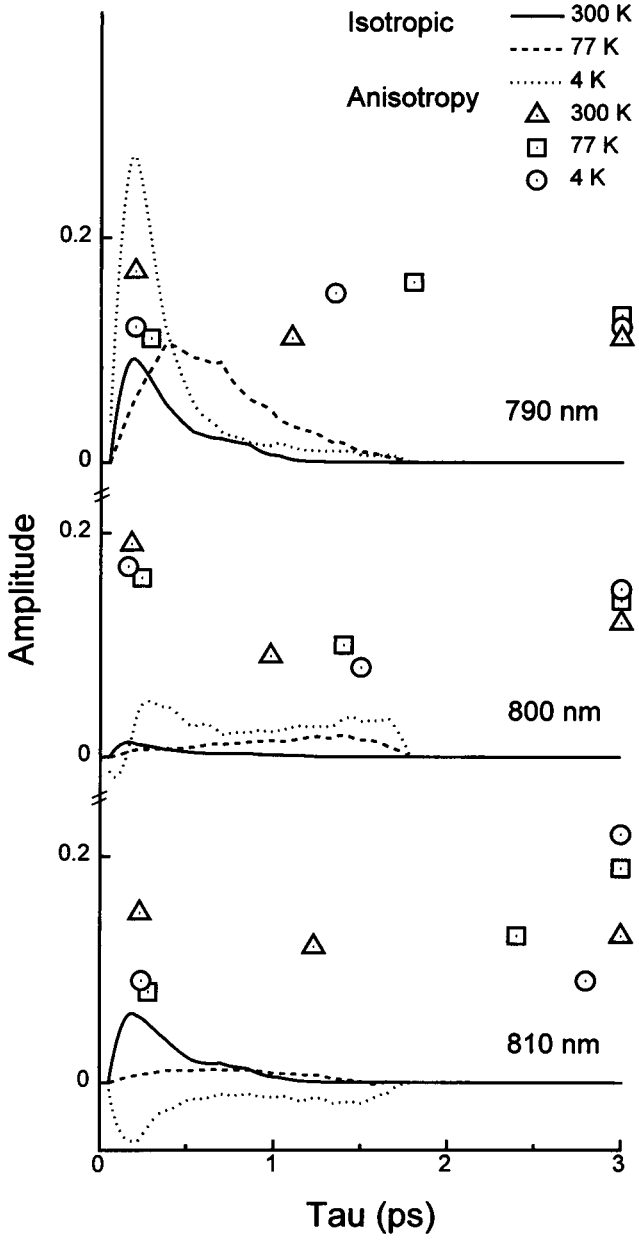

FIGURE 10 Summary of the results of simulations of excitation transfer inside B800 (part of the decay that corresponds to the transfer to B850 is omitted). We have used a hexagonal two-dimensional array of molecules with transition dipole moments randomly oriented in the plane. Inhomogeneous broadening and the spectral width of the laser pulse are taken into account. The lines correspond to distributions of isotropic decay time constants at different recording wavelengths and temperatures. Symbols correspond to the biexponential fits of the calculated anisotropy decays. The leftmost symbols at 3 ps give the corresponding constant level of anisotropy, $r(\infty)$.

three wavelengths at three different temperatures (lines). To visualize better the dynamics inside of the spectrally inhomogeneous B800 band, we have omitted from Fig. 10 the decay component corresponding to the quenching by B850. We cannot directly simulate the distributions of anisotropy decay components, but we have fitted calculated anisotropy decay curves with the sum of two exponentials and a constant background. These results are also presented in Fig. 10 (symbols). The rightmost symbols at 3 ps give the level of the constant background of the anisotropy decays.

First we take a closer look at the isotropic decays. At the blue side at all temperatures one can see fast decay components (300 fs), which are due to the transfer from initially excited high-energy molecules to other molecules that have lower excited-state energy; the 4-K kinetics is the fastest. At 77 K the overall amplitude of the components that is due to the dynamics inside of the IDF is almost the same as at 4 K (in both cases the overall kinetics have an approximately 20% lifetime component, which corresponds to the transfer from B800 to B850), but the lifetime distribution is situated toward much longer times. At 300 K the shape of the lifetime distribution resembles the one at 4 K very much, but the amplitude of the distribution is much smaller (more than 40% of the overall decay amplitude is due to the transfer to B850). At the center of the band the transfer takes place among nearly isoenergetic molecules, and therefore the fast components have very little amplitude and the decay is quite similar at different temperatures. At the red side of the band the kinetics at different temperatures have qualitatively different behavior. At 4 K only a rising component is present, which corresponds to the accumulation of the excitation to the reddest pigments, which give a strong bleaching signal. At 77 K the kinetics at the red edge are almost indistinguishable from the kinetics at the center of the band. At 300 K a remarkable effect appears: because of the uphill energy transfer one can see an apparent fast decay component that makes kinetics at the red edge faster than the corresponding kinetics at the center of the band because at 800 nm initially the full IDF is almost homogeneously excited whereas at 810 nm the excitations are created only at the reddest pigments.

In the anisotropy decay at all wavelengths we see a very fast component of 200 fs, which corresponds to the first jump away from the initially excited molecule. The time constant of this fast component is almost independent of temperature and wavelength. At the same time the amplitude varies considerably with different cases. The amplitude is largest at the center of the band, particularly at 77 and 4 K (note that the isotropic decay had negligible amplitude of the fast component at this spectral region). At these temperatures the homogeneous spectra are so narrow that at both edges of the band it is much less probable that a molecule there has a neighbor with good spectral overlap. This implies not only that the uphill energy transfer is slowed down but that the excitation can also be "trapped" at the blue side of the band because almost all neighbors have so much lower energy that the spectral overlap is relatively small (see Fig. 9). At the center of the band the escape probability is much higher, because there it is much more likely that the initially excited molecule has a neighbor with a good spectral overlap. This effect is a direct analog to the well-known concept of Anderson localization. In our case the localization at the blue edge of the band is not really perfect; the transfer away from there is simply slower than

at the center of the band. At the red edge of the band at 4 K a considerable amount of initially created excitation is really trapped, which is indicated by the high value (>0.2) of the constant level of anisotropy. Here we would like to draw the reader's attention to the fact that even at room temperature at the red edge of the band the constant component of the anisotropy is not the theoretically predicted 0.1 for the two-dimensional system. This effect is due to the finite size of our system. We have 19 molecules, of which 18 provide a constant anisotropy 0.1 and one (the initially excited) provides 0.4. Anisotropy is additive, and one can easily calculate that the constant anisotropy level for our system is approximately 0.12. In our opinion, this effect on the anisotropy of the finite size of a random system is not fully recognized in studies of pigment protein complexes and could give valuable additional information about the structural properties of the studied system.

It has to be pointed out that in the above structural model, if one approximates both anisotropic and isotropic decays with two exponentials, then the fast component of anisotropic decay is always considerably shorter than the corresponding isotropic decay component. Qualitatively one could perhaps expect to find the opposite result (faster isotropic component) if there were some local order in the orientations of transition dipole moments. To investigate this point further we introduced a correlation of orientations of transition dipole moments of molecules in the system and looked for the possibility of finding the necessary level of correlation where the fast component of the anisotropy decay becomes similar to the corresponding isotropic decay that was observed in the experiment.

We used the following algorithm for assigning the orientations of dipole moments of molecules. For the first molecule we give a certain orientation of the dipole moment given by the unit vector $\vec{d}_j$. For the following molecules we use the equation

$$\vec{d}_j = \theta\left[\sum_{i=1}^{j-1} \vec{d}_i \exp\left(-\frac{r_{ij}}{\gamma}\right)\right]^u + (1-\theta)\vec{d}_r, \qquad (3)$$

where $\theta = \exp(-1/\gamma)$. r_{ij} is the distance between molecules i and j; $\vec{d}_j$ is a unit vector oriented randomly in the plane. The superscript u indicates that after summation the vector in brackets has to be normalized to unity. The correlation parameter γ determines the amount of order in the system. If γ is large then θ is close to 1, and the orientation is determined mainly by the first term in Eq. 3; also, inside the sum one can see that molecules that are far from j still make a significant contribution. As a result the dipole moments of molecules are nearly parallel. In the opposite case, if γ is small, then θ is also small, and the orientations of dipole moments are rather random.

It turns out that the time constant of the fastest component of the anisotropy decay does not depend strongly on the correlation parameter γ. However, the amplitudes of different time constants and of the constant background are strongly dependent on γ. This outcome is of course not so surprising because, even if two transition dipole moments are close to parallel (not absolutely parallel), energy transfer from one to another still causes the decrease of the level of anisotropy of the signal with the time constant corresponding to the rate of the transfer. At the same time the amplitude of that decrease depends on the mutual orientation of dipole moments. If molecules have totally random orientation in space, then one transfer step reduces the anisotropy from the initial 0.4 to 0.016 (Agranovich and Galanin, 1982). If there is some correlation of orientations, then the amount of the reduction is different but the time constant is still the same. The subsequent transfer steps of course cause a further reduction of the anisotropy, but it turns out that, if the correlation is introduced as in Eq. 3, then the first step creates a clearly distinctive fast decay component of the anisotropy and the further time constants of the multiexponential fit are much longer (in fact the curve has a general nonexponential behavior). The general expression for the anisotopy after excitation transfer is $r = (3\cos^2\alpha - 1)/5$, where α is the angle between the transition dipole moments of the initially excited molecule and the currently excited molecule.

Inspired by the recent finding that the LH2 antenna has a ringlike structure (McDermott et al., 1995), we have also performed simulations for the model in which all molecules are located on a ring with the transition dipole moments perpendicular to the radius vector and varied the number of molecules in the system (N). If N is large, then neighboring molecules have nearly parallel transition dipole moments, and the first transfer step reduces the anisotropy by a very little amount. It appears that because of the cyclic structure the anisotropy decay is qualitatively different from the previous case of correlated dipole moments. If we fit the anisotropy decay by a single exponential plus a constant background we can clearly see the slowdown of the initial fast anisotropy decay (previously we had mainly a decrease of the amplitude). Strictly speaking, it still has a fast component that corresponds to the single jump and does not depend on N, but the amplitude of this component is very small and could not be distinguished from the decay caused by the subsequent steps. We found that if $N = 8$ then the fast component of anisotropy decay is nearly equal to the single exponential time constant of the isotropic decay, which corresponds to the transfer inside B800. If N is 12, 16, or 20 then the corresponding anisotropy decay times are 1.4, 2.1 or 3.2 times longer than the above-mentioned isotropic decay time. If we compare these results with experimental values for the fast decay components of isotropic and anisotropic decays (0.4 and 0.3 ps, respectively, at 77 K) we can find that the pairwise nearest-neighbor hopping time of B800 molecules at 77 K, averaged over the IDF, is 350 fs. Our measurements also suggest that, if B800 has a ringlike structure, then $N \leq 12$. As can be seen from Fig. 11, LH2 contains nine B800 Bchl a molecules that form a ring and have the Q_y transition dipole moments parallel to the membrane plane.

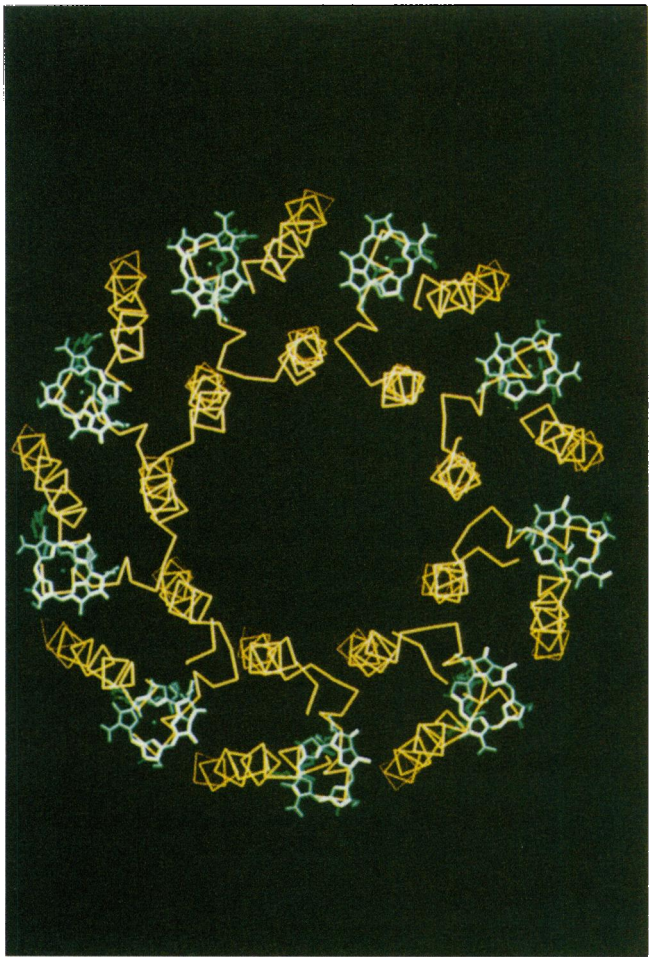

FIGURE 11 Arrangement of the Bchl *a* molecules of B800. Pigments together with β-helixes form an outer ring of the B800–850 complex, whereas α-helixes are in the inner ring.

DISCUSSION

Our interpretations of the experimental data are based on the Förster incoherent excitation transfer theory. Alternatively, exciton relaxation has been applied for describing the ultrafast transfer processes in purple bacteria (Pullerits et al., 1994a; Novoderezhkin and Razjivin, 1994). We point out that for the B800 band all spectroscopic evidence (CD, hole burning) indicates the prevailing monomeric character of that spectral band. Besides, the structural data show that the center-to-center distance between nearest-neighbour B800 Bchl molecules (21 Å) and from these to molecules that belong to B850 (18 Å) is much larger than the center-to-center distance between B850 molecules (~9 Å). Therefore we are justified in treating B800↔B800 and B800→B850 transfer as Förster hopping, whereas for the transfer inside B850 excitonic effects have to be considered seriously.

The pairwise transfer time within B800 seems to be faster than the corresponding transfer from B800 to B850 (at 77 K, 0.35 and 1.8 ps, respectively) in spite of the fact that the distance between B800 molecules is greater than the distance from B800 to B850. This is most likely due to the different spectral overlaps. Between B800 molecules the overlap of donor spectra with phonon wings of acceptors is quite good at 77 K, whereas in the case of B800→B850 transfer the major part of the overlap is coming from the 165-cm^{-1} vibrational mode, which is not very strongly coupled to the electronic transition (Reddy et al., 1991). Consequently the overlap is much smaller for that transfer.

There is much recent evidence that vibrational relaxation and dephasing in antenna complexes of the purple bacteria are not completed on the few-hundred-femtosecond time scale (Chachisvilis et al., 1994, 1995b). This means that the B800↔B800 transfer occurs from a vibrationally hot state (Tehver and Hizhnyakov, 1976). In that case transfer from each optically prepared vibrational level of the donor has to be considered independently, and the resulting kinetics might be multiexponential. However, this is not likely to change our conclusion about the slowdown of the B800↔B800 transfer at the blue wing of the absorption band. Vibrational relaxation can be formally included in Eq. 2 through the time-dependent fluorescence spectrum $f_D(\nu)$. At the initial stage, before the relaxation, emission is resonant to the absorbed light, whereas during the vibrational relaxation it thermalizes to $f_D(\nu)$. In the case of excitation to the blue wing of the absorption band, emission shifts from blue to red. This means that the localization phenomenon at the blue side of the absorption band, which our simulations predict and experiment supports, is even stronger if the hot excitation transfer is properly considered.

Current work and a number of other studies show that there are subpicosecond to picosecond relaxations in large molecules in solution, related to several different processes: solvation, vibrational relaxation, cooling. At low temperature in glass, a substantial part of these motions, which are related to solvation, freezes out, and the relaxations slow down. Whether this is also the case in proteins is not possible to say definitely, because there are very few data on solvation processes and their temperature dependence in proteins. Experiments with Bchl *a* in a protein matrix are in progress to resolve these problems. If other dynamic processes such as vibrational relaxation and electronic dephasing are also present, they are expected to be quite fast. The present measurements show that there are no such relaxations of substantial amplitude in Bchl *a* in the low-temperature glasses. It appears reasonably safe to assume that these intramolecular processes would be present to a similar extent and have approximately the same temporal behavior in glasses and proteins at low temperatures. For our results we therefore presume that the contribution of non-energy-transfer-related relaxation processes to the measured kinetics is small enough not to influence appreciably our main conclusions regarding nearest-neighbor excitation hopping time in B800, excitation localization in the wings of the B800 band, and correlation of B800 anisotropy decay with the LH2 structure. Moreover, all these conclusions are to a large extent based on the anisotropy data, which are expected to be affected very little by intramolecular processes such as vibrational relaxation. Electronic dephasing in an excitonic

system could actually lead to fast anisotropy decay components (Knox and Gülen, 1993). However, in that case one would also expect the initial anisotropy to be above the conventional 0.4, which was not observed in the current measurements. Besides, as we already pointed out, B800 has a basically monomeric character.

The concept of homogeneous and inhomogeneous broadening originates on the basic level from the possibility of separating the time scales of different dynamic processes in the system. At low temperatures when the dynamic fluctuations of the environment of a chromophore are frozen out, the IDF can be seen as truly static. At higher temperatures when the conformational changes in the glass/protein will become faster (spectral diffusion), the picture of the static IDF might not be true any more. We do not have a good physical model to describe that kind of dynamic spectral inhomogeneity, and, as the reference time here is rather short, the excited-state lifetime of 1–2 ps, we consider the IDF to be temperature independent.

B800↔B800 transfer was also observed in the recent fluorescence line-narrowing and hole-burning study at 1.2 K by de Caro et al. (1994). They suggested a time constant of ~900 fs for that process, which is considerably longer than what our direct time-domain experiments yield at 77 K. The difference might be due to the different temperature but also to the complicated decay profile. The fastest components with small amplitudes are not so easy to extract from the frequency-domain experiments.

The value of ~1.8 ps for the B800→B850 transfer time at 77 K is also shorter than what hole-burning experiments suggest at liquid-helium temperatures (Van der Laan et al., 1990; Reddy et al., 1991). This difference is most likely due to the change in the spectral overlap with temperature (Hess et al., 1994). The spectra are narrower and the spectral overlap consequently smaller at lower temperatures. However, the reduction of the energy-transfer rate below 77 K is relatively small; a much bigger decrease occurs between room temperature and 77 K, where the time constant changes from 0.7 to 1.8 ps.

The data presented here reveal a new feature of excitation transfer in spectrally inhomogeneous antenna systems: the localization of excitation at the blue edge of the spectrum at low temperature. This "localization" is not so perfect as it is at the red edge, where excitation gets practically trapped. But still the excitation transfer is slowed down significantly. Our results are in a good agreement with available spectral data and the basic features apparent from the structure of the LH2 complex. It will be interesting to investigate the details of pigment interactions and energy transfer within the complex when the atomic coordinates become available.

This research was financially supported by the Swedish Natural Science Research Council and EEC Research grant SCI*- CT92–0796. RJC acknowledges financial support from the BBSRC.

REFERENCES

Åberg, U., E. Åkesson, J. L. Alvarez, I. Fedchenia, and V. Sundström. 1994. Femtosecond spectral evolution monitoring the bond-twisting event in barrierless isomerization. *Chem. Phys.* 183:269–288.

Avarmaa, R. A., and K. K. Rebane. 1985. High resolution optical spectra of chlorophyll molecules. *Spectrochim. Acta Part A.* 41:1365–1380.

Agranovich, V. M., and M. D. Galanin. 1982. Electronic Excitation Energy Transfer in Condensed Matter. North-Holland, Amsterdam.

Becker, M., V. Nagarajan, D. Middendorf, M. A. Shield, and W. W. Parson. 1990. Excited state properties of bacteriochlorophyll *a* and of bacterial photosynthetic reaction centers as revealed by picosecond absorption studies. *In* Current Research in Photosynthesis. Vol. 1. M. Baltcheffsky, editor. Kluwer Academic Publishers, Dordrecht, The Netherlands. 101–104.

Becker, M., V. Nagarajan, and W. W. Parson. 1991. Properties of the excited-singlet states of bacteriochlorophyll *a* and bacteriopheophytin *a* in polar solvents. *J. Am. Chem. Soc.* 113:6840–6848.

Bergström, H., V. Sundström, R. van Grondelle, E. Åkesson, and T. Gillbro. 1986. Energy transfer within the isolated light-harvesting B800–850 pigment protein complex of *Rhodobacter sphaeroides*. *Biochim. Biophys. Acta.* 852:279–287.

Bergström, H., V. Sundström, R. van Grondelle, T. Gillbro, and R. Cogdell. 1988. Energy transfer dynamics of isolated B800–850 pigment-protein complexes of *Rodobacter sphaeroides* and *Rhodospseudomonas acidophila*. *Biochim. Biophys. Acta.* 936:90–98.

Boonstra, A. F., R. W. Visschers, F. Calkoen, R. van Grondelle, E. F. J. Bruggen, and E. J. Boekema. 1993. Structural characterization of the B800-B850 and B875 light-harvesting antenne complexes from *Rhodobacter sphaeroides* by electron microscopy. *Biochim. Biophys. Acta.* 1142:181–188.

Borisov, A. Yu., A. M. Freiberg. V. I. Godik, K. K. Rebane, and K. E. Timpmann. 1985. Kinetics of picosecond bacteriochlorophyll luminescence in vivo as a function of the reaction center state. *Biochim. Biophys. Acta.* 807:221–229.

Braun, P., and A. Scherz. 1991. Polypeptides and bacteriochlrophyll organization in the light-harvesting complex of *Rhodobacter sphaeroides* R.26-1. *Biochemistry.* 30:5177–5184.

Castner, E. W., Jr. M. Maroncelli, and G. R. Fleming. 1987. Subpicosecond resolution studies of solvation dynamics in polar aprotic and alcohol solvents. *J. Chem. Phys.* 86:1090–1097.

Chachisvilis, M., T. Pullerits, M. R. Jones, C. N. Hunter, and V. Sundström. 1994. Vibrational dynamics in the light-harvesting complexes of the photosynthetic bacterium *Rhodobacter sphaeroides*. *Chem. Phys. Lett.* 224:345–351.

Chachisvilis, M., H. Fidder, and V. Sundström. 1995a. Electronic coherence in pseudo two-colour pump-probe spectroscopy. *Chem. Phys. Lett.* 234:141–150.

Chachisvilis, M., H. Fidder, T. Pullerits, and V. Sundström. 1995b. Coherent nuclear motions in light-harvesting pigments and dye molecules, probed by ultrafast spectroscopy. *J. Raman Spectrosc.* 26:513–522.

De Caro, C., R. W. Vischers, R. van Grondelle, and S. Völker. 1994. Inter- and intraband energy transfer in LH2-antenna complex of purple bacteria. A fluorescence line-narrowing and hole-burning study. *J. Phys. Chem.* 98:10584–10590.

Du, M., S. J. Rosenthal, X. Xie, T. J. DiMagno, M. Schmidt, D. K. Hanson, M. Schiffer, J. R. Norris, and G. R. Fleming. 1982. Femtosecond spontaneous-emission studies of reaction centers from photosynthetic bacteria. *Proc. Natl. Acad. Sci. USA.* 89:8517–8521.

Elsaesser, T., and W. Kaiser. 1991. Vibrational and vibronic relaxation of large polyatomic molecules in liquids. *Annu. Rev. Phys. Chem.* 42: 83–107.

Förster, Th. 1965. Delocalized excitation and excitation transfer. *In* Modern Quantum Chemistry. Vol. III. O. Sinanoglu, editor. Academic Press, Inc., New York. 93–137.

Freiberg, A., V. I. Godik, T. Pullerits, and K. Timpmann. 1989. Picosecond dynamics of direct excitation transfer in spectrally heterogeneous light-harvesting antenna of purple bacteria. *Biochim. Biophys. Acta.* 973: 93–104.

Hess, S., F. Feldshtein, A. Babin, I. Nurgeleev, T. Pullerits, and V. Sundström. 1993. Femtosecond energy transfer within the LH2 periph-

eral antenna of the photosynthetic purple bacteria *Rhodobacter sphaeroides* and *Rhodopseudomonas palustris* LL. *Chem. Phys. Lett.* 216: 247–257.

Hess, S., K. J. Visscher, T. Pullerits, V. Sundström, G. J. S. Fowler, and C. N. Hunter. 1994. Enhanced rates of subpicosecond energy transfer in blue-shifted light-harvesting LH2 mutants of *Rhodobacter sphaeroides*. *Biochemistry.* 33:8300–8305.

Hess, S., M. Chachisvalis, K. Timpmann, M.R. Jones, C.N. Hunter and V. Sunström. 1995. Temporally and spectrally resolved subpicosecond energy transfer within LH2 and from LH2 to LH1 in photosynthetic purple bacteria. *Proc. Natl. Acad. Sci. USA.* In press.

Hunter, C. N., J. D. Pennoyer, J. N. Sturgis, D. Farrely, and R. A. Niederman. 1988. Oligomerization states and associations of light-harvesting pigment-protein complexes of *Rhodobacter sphaeroides* as analyzed by lithium dodecyl sulfate-polyacrylamide gel electrophoresis. *Biochemistry.* 27:3459–3467.

James, D. R., and W. R. Ware. 1985. A fallacy in the interpretation of fluorescence decay parameters. *Chem. Phys. Lett.* 120:455–459.

Jia, Y., D. M. Jonas, T. Joo, Y. Nagasawa, M. J. Lang, and G. R. Fleming. 1995. Observation of ultrafast energy transfer from the accesory bacteriochlorophylls to the special pair in photosynthetic reaction centers. *J. Phys. Chem.* 99:6263–6266.

Kenkre, V. M. 1982. The master equation approach: coherence, energy transfer, annihilation, and relaxation. *In* Exciton Dynamics in Molecular Crystals. Springer-Verlag, Berlin. 1–109.

Knox, R. S., and D. Gülen. 1993. Theory of polarized fluorescence from molecular pairs: Förster transfer at large electronic coupling. *Photochem. Photobiol.* 57:40–43.

Kramer, H. J. M., R. van Grondelle, C. N. Hunter, W. H. J. Westerhuis, and J. Amesz. 1984a. Pigment organization of the B800–850 antenna complex of *Rhodopseudomonas sphaeroides*. *Biochim. Biophys. Acta.* 765: 156–165.

Kramer, H. J. M., J. D. Pennoyer, R. van Grondelle, W. H. S. Westerhuis, R. A. Niederman, and J. Amesz. 1984b. Low-temperature optical properties and pigment organization of the B875 light-harvesting bacteriochlorophyll-protein complex of purple photosynthetic bacteria. *Biochim. Biophys. Acta.* 767:335–344.

Maroncelli, M. J., J. MacInnis, and G. R. Fleming. 1989. Polar solvents dynamics and electron transfer reactions. *Science.* 243:1674–1681.

McDermott, G., S. M. Prince, A. A. Freer, A. M. Hawthornthwaite-Lawless, M. Z. Papiz, R. J. Cogdell, and N. W. Isaacs. 1995. Crystel structure of an integral membrane light-harvesting complex from photosynthetic bacteria. *Nature (London).* 374:517–521.

Novoderezhkin, V. I., and A. P. Razjivin. 1994. Exciton states of the antenna and energy trapping by the reaction center. *Photosynth. Res.* 43:9–15.

Pullerits, T., and A. Freiberg. 1992. Kinetic model of primary energy transfer and trapping in photosythetic membranes. *Biophys. J.* 63: 879–896.

Pullerits, T., M. Chachisvalis, C. N. Jones, C. N. Hunter, and V. Sundström. 1994a. Exciton dynamics in the light-harvesting complexes of *Rhodobacter sphaeroides*. *Chem. Phys. Lett.* 224:355–365.

Pullerits, T., F. van Mourik, R. Monshouwer, R. W. Visschers, and R. van Grondelle. 1994b. Electron-phonon coupling in the B820 subunit form of LH1 studied by temperature dependence of optical spectra. *J. Lumin.* 58:168–171.

Pullerits, T., K. V. Vissher, S. Hess, V. Sundström, A. Frieberg, K. Timpmann, and R. van Grondelle. 1994c. Energy transfer in the inhomogeneously broadened core antenna of purple bacteria: a simultaneous fit of low-intensity picosecond abssorption and fluorescence kinetics. *Biophys. J.* 66:236–248.

Reddy, N. R. S., G. J. Small, M. Siebert, and R. Picorel. 1991. Energy transfer dynamics in the B800–850 antenna complex of *Rhodobacter sphaeroides*: a hole-burning study. *Chem. Phys. Lett* 181:391–399.

Renge, I., K. Mauring, and R. Avarmaa. 1987. Site-selection optical spectra of bacteriochlorophyll and bacteriopheophytin in frozen solutions. *J. Lumin.* 37:207–214.

Shimada, K., M. Mimuro, N. Tamai, and I. Yamazaki. 1989. Excitation energy transfer in *Rhodobacter sphaeroides*, analysed by the time-resolved fluorescence spectroscopy. *Biochim. Biophys. Acta.* 975:72–79.

Shreve, A. P., J. K. Trautman, H. A. Frank, T. G. Owens, and A. C. Albrecht. 1991. Femtosecond energy transfer processes in the B800–850 light-harvesting complex of *Rhodobacter sphaeroides* 2.4.1. *Biochim. Biophys. Acta.* 1051:280–288.

Savikhin, S., and W. S. Struve. 1994. Femtosecond pumpe-probe spectroscopy of bacteriochlorophyll *a* monomers in solution. *Biophys. J.* 67: 2002–2007.

Sundström, V., R. van Grondelle, H. Bergström, E. Åkesson, and T. Gillbro. 1986. Excitation energy transport in the bacteriochlorophyll antenna systems of *Rhodospirillum rubrum* and *Rhodobacter sphaeroides*, studied by low-intensity picosecond absorption spectroscopy. *Biochim. Biophys. Acta.* 851:431–446.

Sundström, V., and R. van Grondelle. 1992. Ultrafast dynamics of excitation energy transfer in Bchl *a*- and Bchl *b*-containing photosynthetic bacteria. *J. Photochem. Photobiol.* 15:141–150.

Sundström, V., and R. van Grondelle. 1995. Kinetics of excitation transfer and trapping in purple bacteria. *In* Anoxygenic Photosynthetis Bacteria. R. E. Blankenship, M. T. Madiga, and C. E. Baner, editors. Kluwer Academic Publishers, Dordrecht, Boston, London. 349–372.

Tehver, I. Y., and V. V. Hizhnyakov. 1976. Radiationless transfer of electronic excitation during vibrational relaxation. *Sov. Phys. JETP.* 42:305–310.

Timpmann, K., A. Frieberg, and V. I. Godik. 1991. Picosecond kinetics of light excitations in photosynthetic purple bacteria in the temperature range of 300–4 K. *Chem. Phys. Lett.* 182:617–622.

Valkunas, L., V. Liuolia, and A. Freiberg. 1991. Picosecond processes in chromatophores at various light intensities. *Photosynth. Res.* 27:83–95.

Van der Laan, H., Th. Schmidt, K. J. Visscher, R. van Grondelle, and S. Völker. 1990. Energy transfer in the B800–850 light-harvesting antenna complex of *Rhodobacter sphaeroides:* a study by spectral hole-burning. *Chem. Phys Lett.* 170:231–238.

Van der Laan, H., C. de Caro, Th. Schmidt, R. W. Visschers, R. van Grondelle, G. J. S. Fowler, C. N. Hunter, and S. Völker. 1993. Excited-state dynamics of mutated antenna complexes of purple bacteria studied by hole-burning. *Chem. Phys. Lett.* 212:569–581.

Van Grondelle, R. 1985. Excitation energy transfer, trapping and annihilation in photosynthetic systems. *Biochem. Biophys. Acta.* 811:147–195.

Van Grondelle, R., H. Bergström, V. Sundström, and T. Gillbro. 1987. Energy transfer within the bacteriochlorofyll antenna of purple bacteria at 77 K, studied by picosecond absorption recovery. *Biochim. Biophys. Acta.* 894:313–326.

Van Mourik, F., A. M. Hawthornthwaite, C. Vonk, M. B. Evans, R. J. Cogdell, V. Sundström, and R. van Grondelle. 1992. Spectroscopic characterization of the low light B800–850 light-harvesting complex of *Rodopseudomonas palustris* strain 2.1.6. *Biochim. Biophys. Acta.* 1140: 85–93.

Visscher, K. J., V. Gulbinas, R. Cogdell, R. van Grondelle, and V. Sundström. 1993. Ultrafast energy transfer within the light-harvesting antenna of photosynthetic purple bacteria. *In* Ultrafast Phenomena. Vol. VIII of Springer Series in Chemical Physics. J.-L. Martin, A. Migus, C. A. Mowren, A. H. Zewail, editors. 55:559–561.

Visschers, R. W., M. C. Chang, F. van Mourik, P. S. Parkes-Loach, B. A. Heller, P. A. Loach, and R. van Grondelle. 1991. Fluorescence polarization and low-temperature absorption spectroscopy of a subunit form of light-harvesting complex I from purple photosynthetic bacteria. *Biochemistry.* 30:5734–5742.

Weaver, J. M., G. E. MacManis, W. Jarzeba, and P. F. Barbara. 1990. Importancy of the fast solvent relaxation components to electron transfer rates: comparisons between barrier-crossing frequencies and subpicosecond time-resolved solvation dynamics. *J. Phys. Chem.* 94:1715–1719.

Zhang, F. G., R. van Grondelle, and V. Sundström. 1992. Pathways of energy flow through the light-harvesting antenna of the photosynthetic purple bacterium *Rhodobacter sphaeroides*. *Biophys. J.* 61:911–920.